# Immobilization of uranyl Schiff base in mesoporous MCM-41

Sushanta K. Badamali[a], Arvind K. Tripathi[a], Dimple P. Dutta[b], Vimal K. Jain[b], and Narendra M. Gupta[a,*]

[a] *Applied Chemistry Division, Bhabha Atomic Research Centre, Trombay, Mumbai 400 085, India*

[b] *Novel Material and Structural Chemistry Division, Bhabha Atomic Research Centre, Trombay, Mumbai 400 085, India*

Received 23 July 2002; accepted 12 September 2002

A uranyl Schiff base complex [$UO_2\{OC_6H_4N{=}C(H)C_6H_4O\}{\cdot}H_2O$] has been immobilized inside the periodic mesopore channels of MCM-41 by the impregnation route. The samples have been characterized by XRD, $N_2$ adsorption/desorption, TG-DTA, DR UV–vis, $^{29}$Si MAS NMR and FTIR techniques. While the host is found to retain its structural integrity, the surface area and the pore volume decrease considerably as a result of the intrapore confinement of complex molecules. The spectroscopy results indicate that the complex molecules are anchored with the silanol groups of MCM-41 via hydrogen bonding.

**KEY WORDS:** MCM-41; uranyl Schiff base; immobilization.

## 1. Introduction

Mesoporous molecular sieves have received much attention during recent years owing to their very high surface area (800–1000 $m^2\,g^{-1}$), tailored pore sizes (20–100 Å) and good thermal stability [1]. These characteristics make mesoporous materials ideal candidates as shape-selective catalysts, as hosts for the heterogenization of homogeneous catalysts and as supports for metal/metal oxide catalysts [2,3]. Also, the internal surface hydroxyl groups in MCM-41 provide convenient anchoring sites on which inorganic metal complexes can be immobilized. The physical entrapment of metal complexes in the micro-/mesopore space provides many advantages, such as shape selectivity, enhanced activity, site isolation, stability, etc., that cannot be realized in the homogeneous phase or using conventional supports. Although recent reports on the catalytic performance of uranium complexes are quite promising [4–6], no report on the heterogenization of uranyl complexes in molecular sieves is available so far. In pursuance of our interest in uranium-based catalysts [7,8], we report here a study of the encapsulation of a uranyl Schiff base complex in MCM-41 silicate molecular sieves. The nature of the host–guest interaction in the ensuing material has been investigated by DR UV–vis, $^{29}$Si MAS NMR and FTIR spectroscopy.

## 2. Experimental

### 2.1. Preparation of ligand [$HOC_6H_4N{=}C(H)C_6H_4OH$]

The ligand was prepared by condensing 2-aminophenol with salicylaldehyde in benzene, according to the procedure reported in the literature [9,10]. The sample was characterized on the basis of chemical analysis (experimental composition: C, 73.0%; H, 5.42%; N, 6.40%; calculated values: C, 73.2%; H, 5.57%; N, 6.57%), melting point (185 °C) and $^1$H NMR in $CDCl_3$ ($\delta$: 7.4–7.0 ppm).

### 2.2. Preparation of uranyl Schiff base complex [$UO_2\{OC_6H_4N{=}C(H)C_6H_4O\}{\cdot}H_2O$]

The uranyl Schiff base was prepared by dropwise addition of a benzene suspension of uranyl acetate, $UO_2(OAc)_2{\cdot}2H_2O$ (772 mg (1.82 mmol) in 25 ml), to a benzene solution of the ligand (388 mg, 1.82 mmol in 25 ml) under constant stirring at room temperature. The solution was evaporated *in vacuo* to give an orange-colored solid (850 mg, 94% yield). The product was characterized as [$UO_2\{OC_6H_4N{=}C(H)C_6H_4O\}{\cdot}H_2O$]. The chemical composition of the product was found to be: C, 32.0%; H, 1.8%; N, 2.7%, against the following values calculated for the above formula: C, 31.3%; H, 2.2%; N, 2.8%.

### 2.3. Complex encapsulation

Mesoporous MCM-41 was synthesized hydrothermally according to the reported procedure [1]. The immobilization of the uranyl Schiff base complex was achieved by the impregnation method. Prior to impregnation, the template-free MCM-41 was heated under vacuum (~$10^{-4}$ torr, 493 K, 5 h) followed by cooling to ambient temperature. The uranyl Schiff base complex (12 mg in 20 ml of $CH_2Cl_2$) was added without any exposure to air and the mass was kept overnight under agitation. The buff-yellow solid was subsequently recovered by evaporating the solvent under ambient conditions. In order to ensure the removal of excess complex from the

---

* To whom correspondence should be addressed.
E-mail: nmgupta@magnum.barc.ernet.in

1011-372X/03/0100-0013/0 © 2003 Plenum Publishing Corporation

external surface, the sample was washed thoroughly with dichloromethane until the filtrate was colorless. The sample was then dried in an air oven at 353 K for 5 h and is referred to as USB/MCM-41 in the text for brevity.

### *2.4. Characterization*

Powder XRD, $N_2$ adsorption/desorption, FTIR, DR UV–vis and $^{29}$Si MAS NMR techniques were employed to characterize the samples. XRD patterns of the samples were recorded in the $2\theta$ region of 1–10° using nickel-filtered Cu$K_\alpha$ radiation in a STOE diffractometer. A Sorptomatic-1990 surface area analyzer was used for $N_2$ adsorption/desorption measurements. Prior to surface area measurements, the samples were evacuated ($\sim 10^{-3}$ torr) at 523 K for 8 h. However, USB/MCM-41 was pretreated at a lower temperature of 373 K in order to preserve the integrity of the loaded complex. The uranium content, as estimated by colorimetry, was found to be ~6.5 wt%. FTIR spectra were recorded in the 4000–400 cm$^{-1}$ region using a JASCO model 610 FTIR spectrometer at a resolution of 4 cm$^{-1}$. For this purpose, KBr pellets of the samples (2 wt%) were employed, and for each spectrum 100 scans were co-added. The UV–vis reflectance spectra were recorded on a Shimadzu UV-260 spectrophotometer. $^{29}$Si MAS NMR spectra were recorded on a Bruker NMR (model DPX 300) spectrometer and the chemical shifts were measured with respect to tetramethylsilane.

## 3. Results and discussion

### *3.1. XRD*

The XRD pattern of the uranyl Schiff base encapsulated in MCM-41 (figure 1) matched closely with that of the parent MCM-41. The presence of well-defined (100), (110) and (200) reflections indicated that the molecular sieves retained their integrity and the crystallinity was preserved after encapsulation.

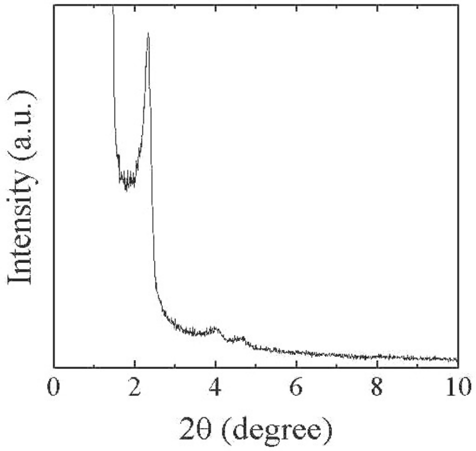

Figure 1. XRD pattern of uranyl Schiff base immobilized in MCM-41.

### *3.2. Surface area and pore size distribution*

The adsorption/desorption isotherms of nitrogen (at 77 K) for both the pristine MCM-41 silica (solid curve) and the USB/MCM-41 sample (dotted curve) are shown in figure 2. The inset shows the pore size distribution, calculated from the desorption branch of the isotherm using the Barrett–Joyner–Halenda (BJH) method. The isotherms of both the samples are of type IV (IUPAC classification [11]), that are typical of mesoporous materials [1,12,13]. The presence of the combined hysteresis loops of type $H_3$ and $H_4$ [11] over the $p/p_o$ range 0.3–1.0 with inflection at $p/p_o$ in the 0.20–0.30 region and at ~0.9 suggest that, along with the slit-shaped mesopores, macropores caused by particle–particle porosity (textural porosity) are also present in both the samples. A summary of the characteristics of the two samples is given in table 1. The decreases in the surface area, pore size and pore volume in the case of USB/MCM-41 (table 1, figure 2 dotted curve) are all indicative of the intrapore confinement of the uranyl Schiff base complex in the mesoporous channel of MCM-41 silica.

### *3.3. UV–vis spectroscopy*

Curves (a) and (b) in figure 3 are the UV–vis spectra of a uranyl Schiff base complex in its free and encapsulated form, respectively. As compared to sharp overlapping bands at around 328, 420, 428, 445, 469, 485 and 504 nm in the UV–vis spectrum of uranyl acetate, arising due to well-reported vibronic transitions within the uranyl group [14,15], the spectrum of the uranyl Schiff base (figure 3(a)) showed a broad band ($\lambda_{max} = 480$ nm) along with some unresolved shoulders at around 274, 320 and 376 nm, which may be a consequence of the closely spaced intraligand/$UO_2^{2+}$ and ligand charge transfer to the uranyl group. This envelope was found to be blue shifted ($\lambda_{max} = 440$ nm) on encapsulation of the complex in MCM-41 (figure 3(b)). The origin of such a shift has been assigned previously to the polarity of the adsorbent surface [16,17]. The mesopore walls of MCM-41 consist exclusively of a dense arrangement of Si–O–Si and Si–O–H groups, which is therefore hydrophilic in nature and may behave like a polar (solid) solvent. It is thus likely that the Si–OH groups are involved in hydrogen bonding with the uranyl oxygen and with the oxygen/nitrogen atoms of the ligand (scheme 1).

### *3.4. FTIR spectroscopy*

Spectra (b) and (c) in figure 4 represent the limited region IR bands of MCM-41 and USB/MCM-41, respectively. Spectrum (a) shows the comparative vibrational bands of the free uranyl Schiff base complex. The IR bands at 933 and 869 cm$^{-1}$ observed in figure 4(a)

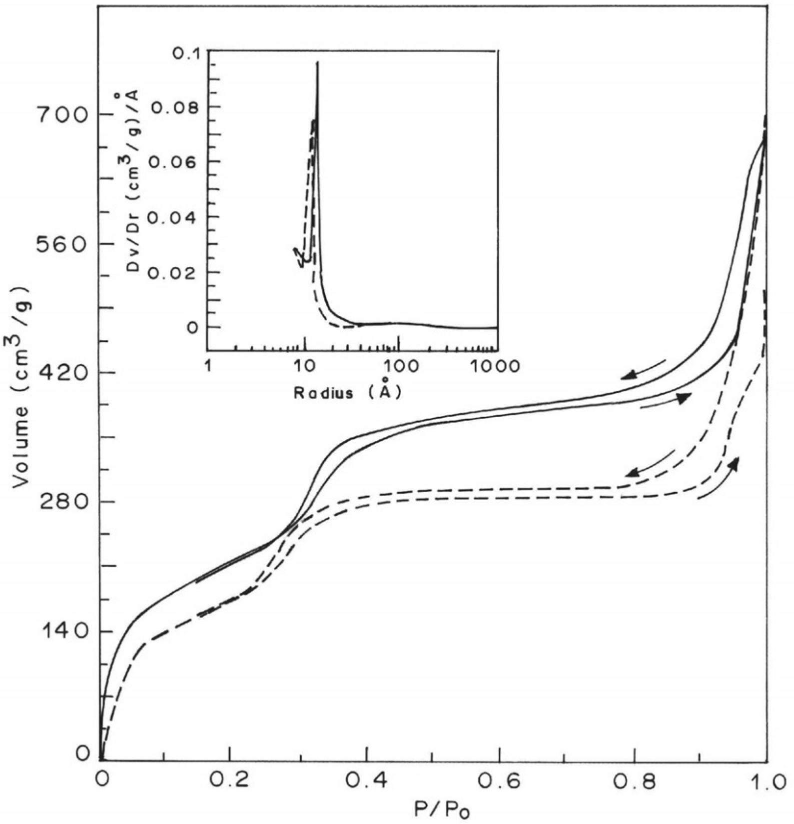

Figure 2. $N_2$ adsorption/desorption isotherm for pristine MCM-41 (solid lines) and USB/MCM-41 (dotted lines). Inset shows the BJH pore size distribution for the two samples.

may be assigned to the asymmetric $\nu_{\mathrm{asym}}$(U=O) and the "infrared forbidden" symmetric stretching $\nu_{\mathrm{asym}}$(U=O) vibrations of the uranyl group, respectively. Such an appearance of the forbidden symmetric vibration has been ascribed previously to the crystal field effect [18]. The assignments for the $\nu$(U=O) vibrations agree with those reported previously for the related complexes [9,10]. Weak overlapping bands at similar frequencies may be discerned in the case of the spectrum of the encapsulated zeolite sample (figure 4(c)), indicating the presence of the uranyl Schiff base complex. Other bands in this region, i.e. at 946 and 916 $\mathrm{cm}^{-1}$ may be attributed to CH bending and the phenyl ring vibrations of the complex [19]. No such features are seen in the host sample (figure 4(b)). A broad band seen in spectra (b) and (c) at 963 $\mathrm{cm}^{-1}$ may be ascribed to ≡Si–$O^-$ defect sites [20]. The blue shift in the $\nu(UO_2^{2+})$ band at 933 $\mathrm{cm}^{-1}$ by ~6 $\mathrm{cm}^{-1}$ in the case of the IR spectrum of USB/MCM-41 as compared to free complex (figure 4(a)) and a similar shift in other bands observed in spectrum (c) may be attributed to the perturbation in the uranyl symmetry due to its interaction with the silicate matrix, as shown in scheme 1.

Table 1
Nitrogen physisorption data for pristine MCM-41 silica and USB/MCM-41 sample

| Sample | $S_{\mathrm{BET}}$, $N_2$ ($\mathrm{m}^2\,\mathrm{g}^{-1}$) | Pore radius, $r_{\mathrm{PN2(BJH)}}$ (Å) | Pore volume ($\mathrm{cm}^3\,\mathrm{g}^{-1}$) |
|---|---|---|---|
| Pristine MCM-41 | 848 | 14.6 | 0.935 |
| USB/MCM-41 | 671 | 13.3 | 0.584 |

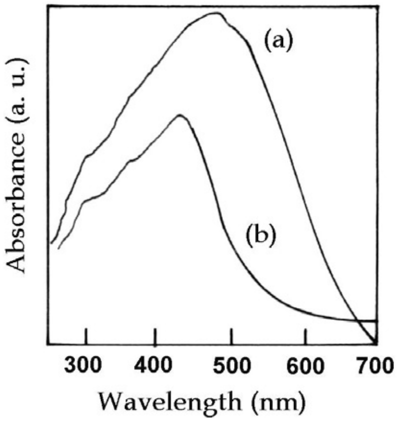

Figure 3. DR UV–vis spectra of uranyl Schiff base complex (a) in free and (b) in encapsulated form in MCM-41.

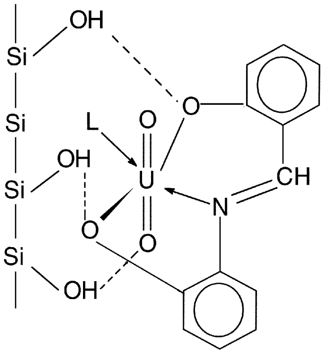

Scheme 1. Schematic of the mode of immobilization of uranyl Schiff base within the inner surface of MCM-41; $L = H_2O$.

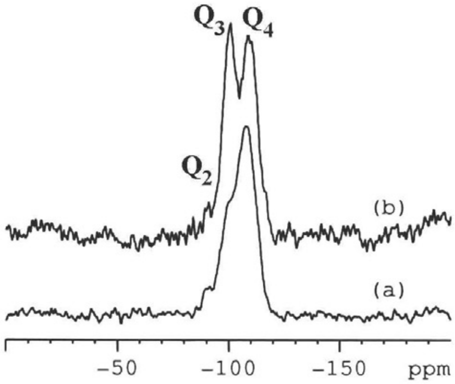

Figure 5. $^{29}$Si MAS NMR spectra of (a) USB/MCM-41 and (b) MCM-41.

### 3.5. NMR spectroscopy

Figure 5 shows the $^{29}$Si MAS NMR spectra of MCM-41 and USB/MCM-41. Signals at $\delta = -90$, $-101$ and $-110$ ppm (figure 5(b)), attributable to $Q_2$, $Q_3$ and $Q_4$ sites of MCM-41 ($Q_n = Si(OSi)_n(OH)_{4-n}$) are in agreement with the reported values [21]. Although the chemical shifts for these sites in USB/MCM-41 (figure 5(a)) are affected only nominally, the peak intensity of the $Q_3$ site is reduced considerably, i.e. from a value of ~47% on a pristine MCM-41 sample to a value of ~34% for USB/MCM-41. These subtle changes indicate again that the hydroxyl protons of SiOH groups ($Q_3$ site) are interacting with the phenolate/uranyl oxygen atoms of the complex (scheme 1). Such effects of the guest molecules on the position and the intensity of MAS

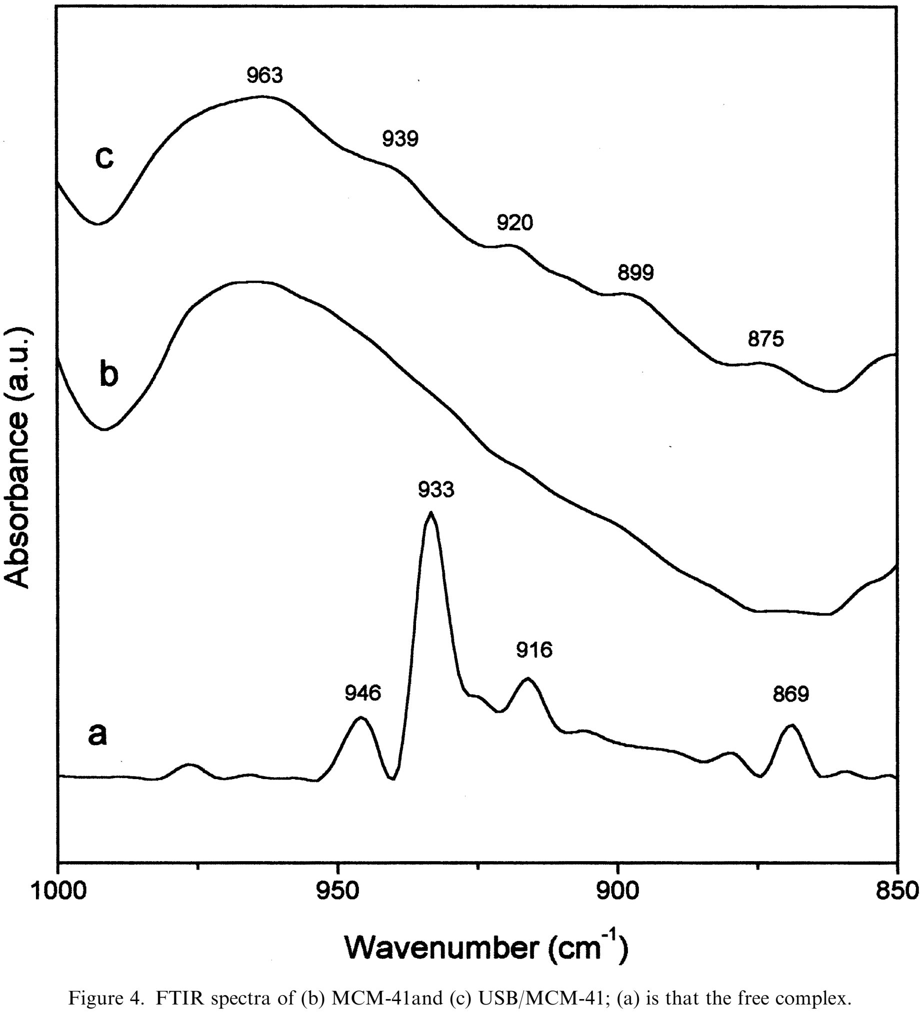

Figure 4. FTIR spectra of (b) MCM-41and (c) USB/MCM-41; (a) is that the free complex.

NMR spectra peaks of MCM-41 have been reported previously [22].

## 4. Conclusion

The present work demonstrates the immobilization of the uranyl Schiff base complex within the mesopores of MCM-41. The complex molecules appear to be hydrogen bonded to the silanol groups ($Q_3$ sites) of the inner surface of MCM-41, at the same time maintaining their integrity.

## Acknowledgments

The authors thank Mr. K.T. Pillai, Fuel Chemistry Division, for surface area and pore size measurements. The help of Mr. V. Sudarsan, NM&SCD, for recording of MAS NMR is gratefully acknowledged. S.K. Badamali thanks the Board of Research in Nuclear Sciences (BRNS-DAE) for a Research Associateship.

## References

[1] J.S. Beck, J.C. Vartuli, W.J. Roth, M.E. Leonowicz, C.T. Kresge, K.D. Schmitt, C.T-W. Chu, D.H. Olson, E.W. Sheppard, S.B. McCullen, J.B. Higgins and J.L. Schlenker, J. Am. Chem. Soc. 114 (1992) 10834; C.T. Kresge, M.E. Leonowicz, W.J. Roth and J.C. Vartuli, Nature 359 (1992) 710.
[2] K. Moller and T. Bein, Chem. Mater. 16 (1998) 2950.
[3] Stein, B.J. Malde and R.C. Schroden, Adv. Mater. 12 (2000) 1403.
[4] J.R. Lacher, J. Schwarz and J.D. Park, J. Org. Chem. 26 (1961) 2536.
[5] R.G. Bowman, R. Nakamura, P.J. Fagan, R.L. Burwell Jr and T.J. Marks, J. Chem. Soc. Chem. Commun. (1981) 257.
[6] G.J. Hutchings, C.S. Heneghan, I.D. Hudson and S.H. Taylor, Nature 384 (1996) 341.
[7] K. Vidya, S.E. Dapurkar, P. Selvam, S.K. Badamali, D. Kumar and N.M. Gupta, J. Mol. Catal. A: Chem. 181 (2002) 91.
[8] K. Vidya, S.E. Dapurkar, P. Selvam, S.K. Badamali and N.M. Gupta, Microporous Mesoporous Mater. 50 (2001) 173.
[9] O.A. Rajan and A. Chakravorty, Inorg. Chim. Acta 50 (1981) 79.
[10] Syamal and K.S. Kale, Inorg. Chem. 18 (1979) 992.
[11] K.S.W. Singh, D.H. Everett, R.A.W. Haul, L. Moscou, R.A. Pierotti, J. Rouquerol and T. Siemieniewska, Pure Appl. Chem. 57 (1985) 603.
[12] C.N. Wu, T.S. Tasi, C.N. Liao and K.J. Chao, Microporous Mater. 7 (1996) 173.
[13] M. Grün, K.K. Unger, A. Matsumoto and K. Tsutsumi, Microporous Mesoporous Mater. 27 (1999) 207.
[14] S.P. McGlynn and J.K. Smith, J. Mol. Spectrosc. 6 (1961) 164.
[15] H.D. Burrows and T.J. Kemp, Chem. Soc. Rev. 3 (1974) 139.
[16] L. Frunza, H. Kosslick, H. Landmesser, E. Hoft and R. Fricke, J. Mol. Catal. A: Chem. 123 (1997) 179.
[17] B. Jezowska-Trzebiatowska and A. Bartecki, Spectrochim. Acta 18 (1962) 799.
[18] H.R. Hoekstra and S. Siegel, J. Inorg. Nucl. Chem. 18 (1961) 154.
[19] H.A. Szymansky, *Interpreted Infrared Spectra*, Vol. 1 (Plenum Press, New York, 1964), p. 80.
[20] C.-Y.Chen, H.-X.. Li and M.E. Davis, Microporous Mater. 2 (1993) 17.
[21] M. Stocker, Stud. Surf. Sci. Catal. 102 (1996) 141.
[22] M.-H. Ryoo and H. Chon, Microporous Mater. 10 (1997) 35.